


Assessment of the electron-proton energy relaxation rates extracted from molecular dynamics simulations in weakly-coupled hydrogen plasmas

Cong-Zhang Gao , Cun-Bo Zhang, Ying Cai, Yong Wu, Zheng-Feng Fan,^{*} Pei Wang,[†] and Jian-Guo Wang
Institute of Applied Physics and Computational Mathematics, Beijing 100088, People's Republic of China



(Received 17 August 2022; accepted 23 December 2022; published 12 January 2023)

Electron-proton energy relaxation rates are assessed using molecular dynamics (MD) simulations in weakly-coupled hydrogen plasmas. To this end, we use various approaches to extract the energy relaxation rate from MD-simulated temperatures, and we find that existing extracting approaches may yield results with a sizable discrepancy larger than the variance between analytical models, which is further verified by well-known case studies. Present results show that two of the extracting approaches can produce identical results, which is attributed to a proper treatment of relaxation evolution. To discriminate the use of various methods, an empirical criterion with respect to initial plasma temperatures is proposed, which can self-consistently explain the cases considered. In addition, for a transient electron-proton plasma, we show that it is possible to extrapolate the Coulomb logarithm from that derived by initial plasma parameters in a single MD calculation, which is reasonably consistent with previous MD data. Our results are helpful to obtain accurate MD-based energy relaxation rates.

DOI: [10.1103/PhysRevE.107.015203](https://doi.org/10.1103/PhysRevE.107.015203)

I. INTRODUCTION

Nonequilibrium two-temperature plasmas [1,2] are created when ions are heated differently from electrons, followed by plasma thermalization to achieve a uniform temperature which is largely dominated by electron-ion collisions. Hence, understanding the electron-ion energy relaxation is important to evaluate the timescale of the nonequilibrium process, which has found broad applications in, e.g., laser ablation [3], shock waves [4,5], and inertial confinement fusion (ICF) [6], for a wide variety of plasma conditions [2,7–11]. Due to the limit of experimental and diagnostic techniques, early experiments [4,7] have only inferred the existence of nonequilibrium two-temperature plasmas by fitting the experimental data with a two-temperature model (TTM) [4,12], thereby acquiring the measured electron-ion energy relaxation rate. In recent years, experimental efforts have been made to diagnose the time-varying temperature of ions and electrons separately in the plasma [2,9,13] (see a recent review for imploding plasmas [14]), which can serve as direct evidence to validate theoretical models of relevance [15–33].

For various plasma conditions, multiple theoretical and numerical treatments, such as the binary collision theory [15,16], quantum kinetic theory [18,20,28], and molecular dynamics (MD) simulations [17,22–26], have been used to account for likely physical effects at different levels of accuracy. Within a classical binary Coulomb collision picture, Landau [15] and Spitzer [16] (LS) proposed the formula of the electron-ion energy relaxation rate, which explicitly depends on the plasma parameters [e.g., the number density of electrons (n_e) and ions (n_i), the ionization state (z), etc.] as

well as the Coulomb logarithm $\ln \Lambda$. Within this model, the key to determining the electron-ion energy relaxation rate is the $\ln \Lambda$. Strictly speaking, the $\ln \Lambda$ is a divergent collisional integral and is usually approximated in practical applications. For convenience, the lower (b_{\min}) and upper (b_{\max}) limits of the integral has been suggested as *ad hoc* cutoffs, such that it can be analytical expressed as $\ln \Lambda = \ln(b_{\max}/b_{\min})$. In order to incorporate the physics of collision, correlation, screening, diffraction, and quantum effects, a lot of variations of b_{\max} and b_{\min} have been developed [17,20,21,24,32,34]. In most cases, b_{\max} represents the Debye screening length $\lambda_D = \sqrt{k_B T_e / (4\pi n_e e^2)}$, and b_{\min} is the shortest distance of approach, $b_c = ze^2 / (k_B T_e)$. In Ref. [34], taking into account the electrons' degeneracy and ions' contribution, b_{\max} was chosen to be the Debye-Hückel screening length λ_{DH} [34]. To roughly consider quantum effects, b_{\min} was represented by the electron thermal wavelength $\lambda_e = \sqrt{2\pi \hbar^2 / (m_e k_B T_e)}$ when $b_c < \lambda_e$. In the Gericke-Murillo-Schlanges (GMS) model [20], b_{\max} is interpolated between λ_D and the radius of ionic sphere $R_{\text{ion}} = (3/4\pi n_i)^{1/3}$, and b_{\min} is interpolated between b_c and λ_e , which contains strong interactions when the dynamical collective mode is dominant. It is to be noted that the GMS model has been validated using a quantum kinetic approach for dense aluminum plasmas. Recently, by using the effective potential theory, the binary collision framework has been extended to include the correlation effects [29], and the predicted relaxation rate showed a favorable agreement with measured data in strong coupling regimes.

Compared to LS-type models, the form of energy relaxation rate becomes quite sophisticated based on the quantum kinetic approach [18,31,33,35,36], though it can describe quantum effects, strong collisions, and collective excitations. If both ionic and electronic motions are treated classically with the inclusion of diffraction, screening, correlation, and

^{*}fan_zhengfeng@iapcm.ac.cn

[†]wangpei@iapcm.ac.cn

collective effects, then the MD approach is well suited for this purpose. As an efficient means, MD simulations have been widely used to mimic the temperature relaxation process between charged particles across coupling regimes [11,17,22–26,37–43]. For a typical MD simulation, the time evolution of temperatures of electrons and protons and their temperature difference can readily be calculated, visibly reflecting how quick electrons and ions relax in the time domain. In this way, MD-simulated temperatures has directly been used to evaluate the effect of screening [26], ionic correlation [28], exchange interaction of electrons [40], temperature anisotropy [44], coupled collective modes [38], and the sign of the electron charge [42] in plasmas, which has significantly deepened our understanding of the physics of electron-ion energy relaxation. However, these tremendous MD temperature data are difficult to be directly used, for instance, in radiation-hydrodynamics simulations [45–48], in which the electron-ion energy relaxation rate is required as a crucial parameter. For this reason, the extraction of the electron-ion energy relaxation rate from MD-simulated temperatures is important [23–25]; it thus needs a reliable extracting approach.

In a previous study, Glosli *et al.* [23] employed the MD method to simulate electron-proton temperature relaxation in dense hydrogen, and they extracted the Coulomb logarithm $\ln \Lambda$ by a direct exponential fitting to the temperature difference of electrons and protons. By comparing with MD-based $\ln \Lambda$, the accuracy of the analytical models was examined and they found that the GMS model and Brown-Preston-Singleton (BPS) model [21] quantitatively followed the MD results for $\ln \Lambda \geq 1$. In a parallel study for the same system, Jeon *et al.* [24] also carried out MD simulations using a screened potential, but the MD technique here was different from that of Glosli *et al.* [23]. In particular, they fitted transformed MD data by using a simple linear function, and their extracted $\ln \Lambda$ agreed reasonably well with the LS model and were larger than those calculated from quantum kinetic theory by $\sim 30\%$. Subsequently, Dimonte and Daligault (DD) [25] presented MD results for positron-proton plasmas in a wide range of coupling regimes. Although their MD setups were generally consistent with those in Ref. [23], they fitted MD temperatures to three different analytical solutions and sorted out the value that provides the best fitting to the temperature difference. In this way, they have established an analytical relationship between $\ln \Lambda$ and the plasma parameter g , i.e., $\ln \Lambda = \ln(1 + 0.7/g)$ (hereafter, we entitle it the DD model), where g is defined as a ratio of the Coulomb energy of electrons and ions at a distance of λ_D to the thermal energy, which is simply reduced to the ratio of b_c to λ_D . It is found that it precisely follows the BPS model for weakly coupled plasmas.

As described above, there have been several different extracting approaches used in previous MD simulations [23–25], where the authors used to choose one of the extracting methods in their favor. In this situation, a question raised is whether or not various extracting approaches can yield convergent results for the same set of plasma parameters, which is quite essential. If the discrepancy from extracting approaches remains higher than the statistical error of MD simulations (3%–5%), one must work with caution to obtain reliable energy relaxation rates. In a recent study [45], Xu and Hu have shown that a discrepancy of $\sim 5\%$ – 15% in the electron-

ion energy relaxation rates between analytical models would result in substantial variances for the neutron yield in ICF simulations, which has obviously pointed out the importance of the accuracy of the electron-ion energy relaxation rate for ICF implosion performance. We shall show in the following that in certain cases, electron-proton energy relaxation rates extracted by various approaches will differ significantly with a discrepancy that is comparable or even larger than that in Ref. [45]. On the other hand, MD-extracted energy relaxation rates typically serve as the benchmark in the classical limit, e.g., Vorberger and Gericke [35] have directly cited previous MD results to compare with quantum kinetic theory in order to examine the emergence of coupled collective modes in MD simulations. Hence, incorrect assessment of electron-ion energy relaxation rates in MD simulations might inhibit the evaluation of newly developed theoretical models.

As can be seen, a general agreement among existing extracting approaches has not yet been reached for MD simulations, though they have already been used in many studies over the years. In this paper, we provide a definite answer to this problem in weakly-coupled hydrogen plasmas. The objective of the work is to show the impact of extracting approaches of MD simulations on the $\ln \Lambda$, e.g., clarifying whether existing extracting approaches are convergent. Our results show that two of the extracting approaches always yield identical results, while various extracting approaches are convergent only in particular cases. Furthermore, a series of case studies in Refs. [23–25] has been reexamined. And in most cases, we find that extracting approaches result in appreciable uncertainties, which largely exceed the MD simulations' statistical error. To discriminate various extracting approaches, we present an empirical criterion of initial plasma temperatures. Finally, combined with two of the extracting approaches, we show that it is possible to extrapolate other Coulomb logarithms in a single MD calculation, which agrees well with independent MD simulations by varying plasma parameters.

The article is arranged into the following parts. Section II briefly introduces key aspects of MD simulations and illustrates three extracting approaches in more detail. Section III presents systematic MD results and analyzes the applicability of extracting approaches. Finally, a conclusion is drawn in Sec. IV.

II. THEORETICAL METHODS

A. Details of MD simulations

In the present work, the energy relaxation process between electrons and protons in weakly-coupled hydrogen plasmas is simulated by using classical molecular dynamics [49]. A collection of charged particles is restrained inside a cubic domain. Periodic boundary conditions are used in the microcanonical ensemble. The Coulomb force acted upon each particle is directly computed within a large radius centered at the desired particle, i.e., $R_0 = 50$ bohr, which suffices to yield convergent results in the present study. The interaction between electron and proton is described by a quantum statistical potential (QSP) [17,50,51], approximately accounting for the quantum diffraction effect in Coulomb collisions [50],

thereby avoiding the numerical divergence at short distances for electron-proton pairs. Newton's equations of motion are numerically integrated using the velocity-Verlet algorithm. A fixed time step is adopted, ranging from 10^{-7} for an initial temperature of electrons, $T_e^0 \sim \text{keV}$, to 10^{-4} femtoseconds (fs) for $T_e^0 \sim$ a few tens of eV, which is small enough to conserve the total energy ($\Delta E/E \leq 0.1\%$).

In MD simulations, the instantaneous temperature of the plasmas is computed by $T_\alpha(t) = m_\alpha / 3k_B N_\alpha \sum_{j=1}^{N_\alpha} \mathbf{v}_j^2(t)$, where the index α denotes the electron (e) or proton (p) and thus m_α is the corresponding mass. \mathbf{v}_j is the velocity of the j th particle of species α , and N_α is the total number of species α . k_B is the Boltzmann constant. To obtain an initial nonequilibrium plasma with disparate temperatures of electrons and protons ($T_e^0 \neq T_p^0$), we have performed the following three steps. First, a large number of particles is generated with random positions in the simulation cell, and initial particle velocities are randomly sampled from the Maxwell-Boltzmann distribution at room temperature. Second, two Langevin thermostats [52] are separately applied for electrons and protons in order to rapidly heat them up to different temperatures. To ensure the particles of the same kind are fully relaxed, it continuously evolves more than 10^5 time steps. In this way, the two-temperature electron-proton plasma can be well prepared. Finally, by removing external thermostats, the system evolves freely via Coulomb collisions during which charged particles' collisions, diffraction, correlation, and screening are included self-consistently. Thermal equilibrium is achieved with a common temperature for both electrons and ions. Within this approach, we have been able to obtain consistent results in previous studies [23–25,40].

To obtain statistically reliable MD data, we used more than 10^5 electrons and 10^5 protons for each MD simulation. By varying the initial positions of the particles, it is found that the uncertainty of $\ln \Lambda$ remains less than 5% (see the Appendix). In the considered regime, it is a rather small statistical error, compared to the discrepancy seen among various analytical models of $\ln \Lambda$. For this reason, multiple independent simulations sampled with varied initial phase spaces are unnecessary in our study. In addition, the ion mass scaling technique is employed to accelerate the entire relaxation process; specifically, in most simulations, the mass ratio of protons to electrons is 10^2 . The impact of the proton's mass has also been examined. It should be noted that in this study, MD-simulated energy relaxation rates have been rescaled to the real mass ratio of protons to electrons, which are the results presented in the following.

B. Determination of energy relaxation rate

In our study, the key quantity is the electron-ion energy relaxation rate ω_{ei} , which is typically formulated as

$$\omega_{ei} = \frac{4k_B \sqrt{2\pi m_i m_e n_i n_e z^2} e^4}{(m_e k_B T_i + m_i k_B T_e)^{\frac{3}{2}}} \ln \Lambda = \omega_{ei}^0 \ln \Lambda, \quad (1)$$

where ω_{ei}^0 is a prefactor, i.e., $\omega_{ei}^0 = 4k_B \sqrt{2\pi m_i m_e n_i n_e z^2} e^4 (m_e k_B T_i + m_i k_B T_e)^{-\frac{3}{2}}$. $m_i(m_e)$, $z(e)$, $n_i(n_e)$, and $T_i(T_e)$ represent the mass, charge, number density, and temperature of the ions (electrons), respectively. The

number density satisfies the relation of $n_e = zn_i$ due to the global charge neutrality of the plasma. In the following, we briefly summarize three extracting schemes widely used in MD simulations. Without loss of generality, the extracting approach will be introduced for the plasma with an ionization state of z . For the hydrogen plasmas ($z = 1$) considered here, it is reduced to the electron-proton energy relaxation rate ω_{ep} . It is to be noted that various schemes are distinguished by either different simulation methods of identical plasma conditions or different fitting procedures of identical MD data.

1. Full relaxation dynamics

Assume that electrons and ions have distinct initial temperatures, e.g., $T_e^0 > T_i^0$, and that they would fully relax towards a common temperature T_{eq} . This is described by the following equations:

$$\frac{dT_e}{dt} = -v_{ei}(T_e - T_i) = -\frac{1}{\tau_{ei}}(T_e - T_i), \quad (2a)$$

$$\frac{dT_i}{dt} = -v_{ie}(T_i - T_e) = -\frac{1}{\tau_{ie}}(T_i - T_e), \quad (2b)$$

where the notation of the time variable t in T_e and T_i is neglected for simplicity, and the temperature relaxation rate v is defined as

$$v_{ei} = \frac{8}{3} \frac{\sqrt{2\pi m_i m_e n_i z^2} e^4}{(k_B T_i m_e + k_B T_e m_i)^{\frac{3}{2}}} \ln \Lambda = v_0 \ln \Lambda, \quad (3)$$

where v_0 is a prefactor. The temperature and energy relaxation rate is connected by the relationship of $\omega_{ei} = 3/2 k_B n_e v_{ei}$. For hydrogen plasmas ($z = 1$), the relation of $v_{ei} = v_{ie}$ is satisfied. $\tau_{ei}(\tau_{ie})$ is referred to as the relaxation time of electrons (ions). According to Eq. (2), the evolution of the temperature difference $\Delta T(t)$ [defined as $\Delta T(t) = |T_e(t) - T_i(t)|$] obeys

$$\frac{d\Delta T(t)}{dt} = -(v_{ei} + v_{ie})\Delta T(t) = -v^*\Delta T(t), \quad (4)$$

in which the effective temperature relaxation rate is defined as $v^* = (v_{ei} + v_{ie}) = (z + 1)v_{ei}$, and its reciprocal τ^* is the relaxation time that was typically analyzed. By integrating Eq. (4), $\Delta T(t)$ can be analytically written as

$$\Delta T(t) = \Delta T(t=0) \exp \left[-\int_0^t v^*(t') dt' \right]. \quad (5)$$

In previous studies [23,24,40], it was usually assumed that the temperature relaxation rate is linked to the initial plasma parameters, so its time dependency was approximately neglected. Along this line, by using a time-independent effective relaxation rate, a simplified expression $\Delta T(t) = \Delta T(t=0) \exp(-v^*t)$ can be attained. If data of ΔT are available, for instance, calculated in MD simulations, then v^* (thus v_{ei}) can be determined. As a result, the Coulomb logarithm is given as

$$(\ln \Lambda)_{\text{MD}} = \frac{v^*}{(z + 1)v_0} = \frac{1}{(z + 1)v_0 \tau^*}. \quad (6)$$

Obviously, $\ln \Lambda$ is associated with the exponential fitting to full relaxation dynamics data.

An illustration of this approach is shown in Fig. 1(a) for hydrogen plasmas initially with $n_i = n_e = 10^{22} \text{ cm}^{-3}$, $T_e^0 =$

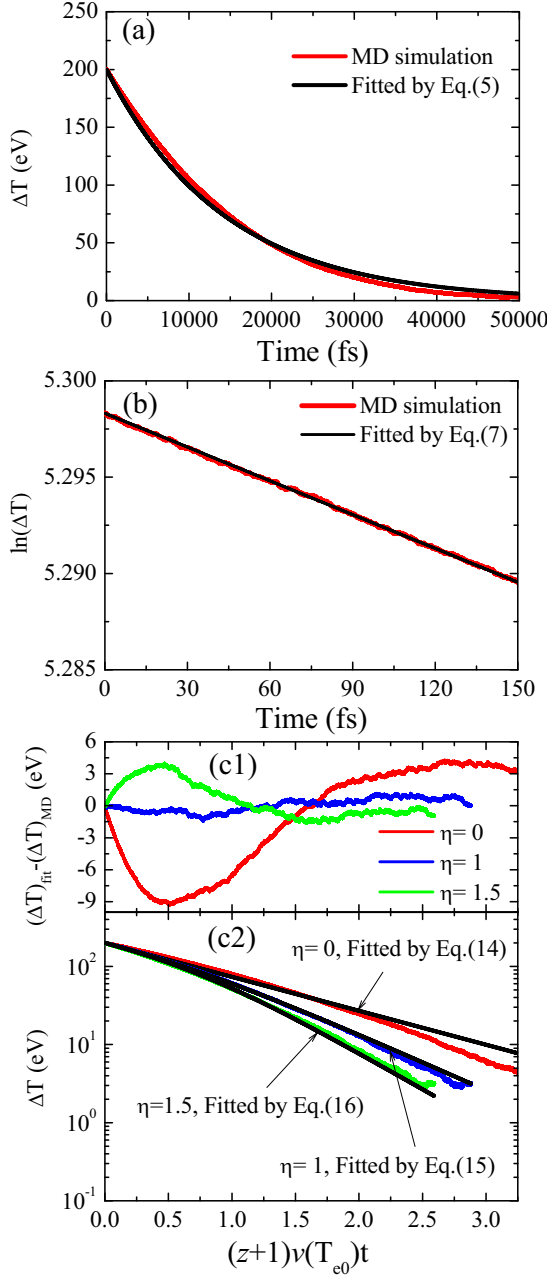


FIG. 1. Comparison of MD simulation results with fitted results by various schemes. (a) Full relaxation dynamics, (b) partial relaxation dynamics, (c) optimal fitting procedure. Note that (b) employs a logarithmic y axis. In order to facilitate the comparison between fitted and MD results, (c1) shows their difference. More details can be found in the main text.

250 eV, and $T_i^0 = 50$ eV; see case C in Table I. For this case, we used 10^5 electrons and 10^5 protons in the MD simulations. The thermal equilibrium is nearly reached with $T_{eq} \approx 150$ eV. If $\Delta T(t)$ computed from MD simulations is fitted by Eq. (5), we obtain $\nu^* = 7.0 \times 10^{-5}$ fs $^{-1}$, and then, based on Eq. (6), the calculated $\ln \Lambda$ is 4.38. According to Eq. (1), we obtain the electron-proton energy relaxation rate $\omega_{ei} = 0.72 \times 10^{16}$ W/(K m 3).

2. Partial relaxation dynamics

As full relaxation dynamics calculations are computationally demanding in most cases, an alternative approach is to perform early relaxation simulations, which requires only a fraction of the total simulation time of full relaxation. To mitigate the statistical fluctuation, partial relaxation simulations call for a substantial number of particles, e.g., at least 10^6 electrons and 10^6 protons [24]. The temperature difference follows an exponential attenuation law [see Eq. (5)], which can be transformed into a linear relation,

$$\ln[\Delta T(t)] = At + B, \quad (7)$$

with the slope $A = -1/\tau_{\text{fit}}$ and the intercept $B = \ln[\Delta T(t = 0)]$. The unknown coefficients in Eq. (7) can be determined by fitting to the MD results [see Fig. 1(b)] and then the electron-proton energy relaxation rate can be computed.

For weakly-coupled plasmas, the electron energy relaxation equation is written as

$$\frac{dE_e}{dt} = \frac{3}{2} k_B n_e \frac{dT_e}{dt} = -\omega_{ei}(T_e - T_i). \quad (8)$$

By substituting Eq. (2a) into it, it arrives at

$$\omega_{ei}^{\text{MD}} = \frac{3k_B n_e}{2(z+1)\tau_{\text{fit}}}. \quad (9)$$

According to the definition in Eq. (1), the Coulomb logarithm is calculated by

$$(\ln \Lambda)_{\text{MD}} = \frac{\omega_{ei}^{\text{MD}}}{\omega_{ei}^0} = \frac{3k_B n_e}{2(z+1)\omega_{ei}^0 \tau_{\text{fit}}}. \quad (10)$$

It should be noted that the fitting procedure utilized in full and partial relaxation dynamics is physically equivalent, but they rely on distinct MD simulations. Figure 1(b) presents results still for case C in Table I. Here, MD simulations are run for 10^6 electrons and 10^6 protons; thereby, the temperature fluctuation is properly suppressed within less than 200 fs, which is far from the equilibrium time. Based on Eq. (7), a linear fit is employed, showing a fairly good agreement with the MD data. The fitted relaxation time is $\tau_{\text{fit}} = 17109.3$ fs. Upon the use of Eqs. (9) and (10), $\ln \Lambda$ is calculated as 3.65, and the electron-proton energy relaxation rate attains $\omega_{ei} = 0.6 \times 10^{16}$ W/(K m 3).

3. Optimal fitting procedure

For a conventional description of electron-proton temperature relaxation, it supposes that the relaxation rate depends only on the initial plasma conditions, as has been formulated in Eq. (6), which may be inappropriate in certain situations. To consider the possible temperature-dependent relaxation rate, the temperature relaxation equation for electrons is modified as [25]

$$\frac{dT_e}{dt} = -\nu_{ei}(T_e^0) \left(\frac{T_e}{T_e^0} \right)^{-\eta} (T_e - T_i). \quad (11)$$

To determine the choice of η , it is assumed that the temperature-dependent relaxation rate $\nu_{ei}(T_e)$ has the same power as $\nu_{ei}(T_e^0)$, but is divided into different components T_e^0 and T_e , i.e., $\nu_{ei}(T_e) \propto (T_e^0)^{-1.5+\eta} (T_e)^{-\eta}$. It is obvious that it is exactly reduced to $\nu_{ei}(T_e^0)$ for T_e approaching T_e^0 . Typically,

TABLE I. Electron-proton energy relaxation rates [in units of $W/(K m^3)$] extracted from MD simulations (S_1 to S_3 in the sixth to eighth columns stand for three extracting approaches in sequence described in Sec. II B) and calculated by well-established analytical models [15,16,20,21,25] (from the ninth to 12th columns). The numbers included in brackets denote the power of 10. The first column labels the cases under study. The number density of electrons (n_e) and ions (n_i), initial electron (T_e^0), and ion (T_i^0) temperatures are arranged into the second to fifth columns. For cases A–C, the electrons are hotter than the ions, with $n_i = n_e = 1 \times 10^{22} \text{ cm}^{-3}$. For cases D–F, the situation is reversed for $n_i = n_e = 3.35 \times 10^{22} \text{ cm}^{-3}$.

Case	n_e cm^{-3}	n_i cm^{-3}	T_e^0 eV	T_i^0 eV	$\omega_{ei}^{\text{MD}}, W/(K m^3)$			Analytical $\omega_{ei}, W/(K m^3)$			
					S_1	S_2	S_3	LS [15,16]	GMS [20]	BPS [21]	DD [25]
A			58	50	0.34(17)	0.33(17)	0.32(17)	0.27(17)	0.45(17)	0.39(17)	0.42(17)
B	10^{22}	10^{22}	80	50	0.24(17)	0.23(17)	0.22(17)	0.20(17)	0.31(17)	0.28(17)	0.30(17)
C			250	50	0.72(16)	0.60(16)	0.60(16)	0.54(16)	0.79(16)	0.71(16)	0.82(16)
D			50	80	0.27(18)	0.31(18)	0.31(18)	0.22(18)	0.48(18)	0.39(18)	0.43(18)
E	3.35×10^{22}	3.35×10^{22}	50	500	0.18(18)	0.26(18)	0.26(18)	0.22(18)	0.47(18)	0.39(18)	0.43(18)
F			50	1000	0.05(18)	0.25(18)	0.25(18)	0.22(18)	0.47(18)	0.39(18)	0.42(18)

we suppose that the exponential factors of two components are negative or zero, i.e., $(-1.5 + \eta) \leq 0$ and $-\eta \leq 0$, such that $0 \leq \eta \leq 1.5$ is obtained. For several specific η values, it is analytically solvable with multiple mathematical manipulations.

For $\eta = 0$, the solution is

$$T_e(t) = T_{eq} + (T_e^0 - T_{eq}) \exp[-\nu_{ei}(T_e^0)(z+1)t], \quad (12)$$

where the equilibrium temperature is given by

$$T_{eq} = \frac{zT_e^0 + T_i^0}{z+1}. \quad (13)$$

For consistency with the formulation of other η , Eq. (12) is rewritten as

$$\nu_{ei}(T_e^0)(z+1)t = \ln \left[\frac{T_{eq} - T_e^0}{T_{eq} - T_e(t)} \right]. \quad (14)$$

Similarly, for $\eta = 1$, it yields

$$\nu_{ei}(T_e^0)(z+1)t = 1 - \frac{T_e(t)}{T_e^0} + \frac{T_{eq}}{T_e^0} \ln \left[\frac{T_{eq} - T_e^0}{T_{eq} - T_e(t)} \right], \quad (15)$$

and for $\eta = 1.5$, we obtain

$$\nu_{ei}(T_e^0)(z+1)t = \left(\frac{T_{eq}}{T_e^0} \right)^{\frac{3}{2}} \left[\ln \left(\frac{\sqrt{\frac{T}{T_{eq}}} + 1}{\sqrt{\frac{T}{T_{eq}}} - 1} \right) - 2 \left(\frac{T}{T_{eq}} \right)^{\frac{1}{2}} - \frac{2}{3} \left(\frac{T}{T_{eq}} \right)^{\frac{3}{2}} \right]_{T=T_e^0}^{T=T_e(t)}. \quad (16)$$

To acquire $\nu_{ei}(T_e^0)$, time-dependent electron temperatures $T_e(t)$ computed in MD simulations are, respectively, fitted by Eqs. (14)–(16). If done so, it is straightforward to calculate the analytical $\Delta T(t)$ for $\eta = 0, 1, 1.5$ according to fitted $\nu_{ei}(T_e^0)$, where the total kinetic energy is assumed to be conserved. This is reasonable for weakly-coupled plasmas in the present study, but remains questionable for strongly-coupled plasmas. The solution with the optimal fitting to $\Delta T(t)$ will be considered as the desirable result for plasmas under study. Finally,

the Coulomb logarithm can be computed using Eq. (3),

$$(\ln \Lambda)_{\text{MD}} = \frac{\nu_{ei}^{\text{MD}}}{\nu_0}. \quad (17)$$

Figure 1(c) exemplifies the optimal fitting approach for case C. Figure 1(c1) examines the difference between MD electron-proton temperature differences and its fitted values for various η factors, and Fig. 1(c2) directly compares the electron-proton temperature difference between MD and fitted results. Applying Eqs. (14)–(16) to fit the MD simulation data, the fitted ν_{ei} are 3.62×10^{-5} , 2.89×10^{-5} , and $2.6 \times 10^{-5} \text{ fs}^{-1}$, respectively. Figure 1(c1) clearly shows that $\eta = 1$ yields the most favorable agreement, corresponding to a value of $\ln \Lambda = 3.61$. Hence, the electron-proton energy relaxation rate $\omega_{ei} = 0.6 \times 10^{16} \text{ W}/(K m^3)$ is determined.

III. RESULTS AND DISCUSSION

A. Comparison with analytical models

We first show the impact of the extracting approaches on the electron-proton energy relaxation rates. For this purpose, we focus on the six cases which can be grouped into two sets: (1) A–C cases for $T_e^0 > T_i^0$, specifically, $T_i^0 = 50 \text{ eV}$ and $T_e^0 = 58, 80, \text{ and } 250 \text{ eV}$; and (2) D–F cases for $T_e^0 < T_i^0$, with $T_e^0 = 50 \text{ eV}$ and $T_i^0 = 80, 500, \text{ and } 1000 \text{ eV}$. The plasma conditions, i.e., weakly-coupled plasmas, are well suited for MD simulations. As for the extracting approach, it should be mentioned that in all the cases considered in this work, we have used $\eta = 0, 1, 1.5$ in the optimal fitting procedure to fit the MD data separately, and it is found that $\eta = 1$ always gives the most satisfactory fitted results, which are summarized in Table I and Fig. 2. Three features are immediately observed in Table I. First, the results given by the S_2 method (partial relaxation dynamics) in all cases are identical to S_3 (optimal fitting procedure), implying that the two extracting approaches are generally convergent regardless of plasma conditions. Second, with increasing the temperature difference, the S_1 method (full relaxation dynamics) largely overestimates or underestimates the rates compared to the other two methods. For instance, the value, computed by the S_1 method, is higher (lower) than that by the S_2 and S_3 methods by $\sim 20\%$ ($\sim 80\%$) for case C (F), which is much larger than the statistical error of MD

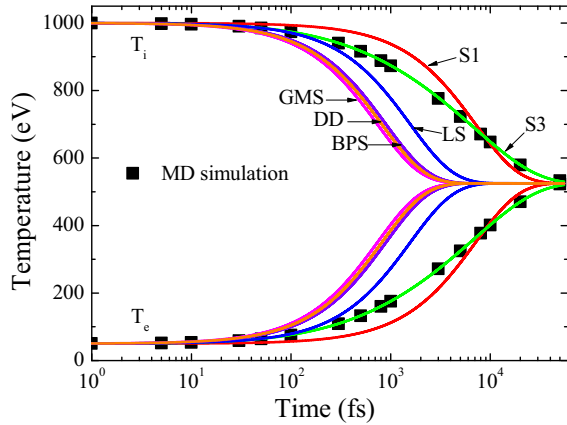


FIG. 2. Time evolution of the electron and ion temperature for MD simulations (solid square symbols), together with the fitting results of full relaxation dynamics (S1, red curves) and optimal fitting procedure (S3, green curves). For comparison, the analytical LS (blue curves), GMS (pink curves), BPS (purple curves), and DD (orange curves) results are shown. This illustration corresponds to case F in Table I

simulations (~5%). Third, the three extracting methods are all convergent, i.e., the deviation is below the MD statistical error, only for small temperature differences (cases A and B), as expected.

In order to further illustrate the results deviation due to the various extracting approaches, results from the LS, GMS, BPS, and DD analytical models are included in Table I. It should be noted that these four analytical models has been used in Ref. [45], in which their influence on the ICF implosion performance was evaluated. We have the impression that for electron-proton energy relaxation rates extracted from MD temperatures in certain cases, incorrect assessment might bring considerable errors which are comparable to or larger than the variance between analytical models. For case C, the deviation due to the various extracting approaches is $0.12 \times 10^{16} \text{ W}/(\text{K m}^3)$, which is comparable to the deviation between the BPS and DD models, larger than that between the GMS and BPS models, but remains smaller than that between the LS and other models. The comparison is even pronounced for case F. All in all, we believe that the estimated error in the electron-proton energy relaxation rates using the extracting approaches may be far from negligible.

Since the MD simulations can directly provide the temperature of electrons and protons, it is instructive to make a comparison between the fitted results and MD temperatures. As an illustrative example, we select case F with very hot protons and cold electrons, which is useful to test the validity of the various extracting approaches. Figure 2 presents the calculated results alongside the analytical models. As can be seen in the entire time evolution, the S₃ method (optimal fitting procedure) provides the best agreement with the MD simulations. In contrast, other methods and models follow the MD temperatures only before 30 fs. From the figure, we see that the S₁ method (full relaxation dynamics) predicts a much slower electron-proton relaxation process than MD simulations, yielding a relaxation time of 7123.2 fs, which

is longer than that of MD by about a factor of 5. This is in accordance with the results listed in Table I.

Obviously, for analytical models, it predicts faster relaxations than MD results, in which the GMS, BPS, and DD models show very similar results. We notice that these results are at variance with the Glosli *et al.* [23] results, where the BPS model was favorable. This can be attributed to the difference of plasma conditions. In Ref. [23], during temperature relaxation, the electron temperature is decreased by 43%, resulting in a variation of the plasma parameter g between 0.28 and 0.66, a coupling regime with slow variations of relaxation rates [25,37], while in the present study, for case F, the electron temperature is increased by a factor of 9.5 from the initial to equilibrium state, which leads to a broad alteration of g by orders of magnitude and thus the relaxation rate is violently modified. As a result, the BPS model fails to predict the MD results in our case. We shall return to this point later in Sec. III C.

B. Case studies revisited

In this section, we shall reexamine a variety of case studies in hydrogen plasmas reported in prior calculations [23–25]. Since numerical setups differ in Refs. [23–25] and our simulations, such as particle numbers and time steps, we do not intend to benchmark against their numerical results. Instead, we would like to figure out, for the plasma conditions involved in these studies, whether the energy relaxation rates are considerably affected by the extracting approaches. As the S₂ and S₃ methods can yield identical results (see Table I), we adopt either of them to compare with the S₁ method.

We calculated nine cases considered in the work of Glosli *et al.* [23], with the temperature ranging from 10 to 600 eV and the electron density from 10^{20} to 10^{24} cm^{-3} . Our results are collected in Table II. We see that in the majority of cases, the relative errors due to various extracting approaches are appreciable, i.e., higher than 15%, which comfortably exceeds the statistical error of MD simulations. This observation does not contradict that in Ref. [23] because Glosli *et al.* used a rather small particle number, which is at least two orders of magnitude smaller than the present calculations. Therefore, it is not surprising that their results were often accompanied by sizable statistical errors, as clearly seen in Fig. 2 in Ref. [23]. For example, for case 1, Ref. [23] obtained an absolute statistical error of 19.4%–31.6%, which entirely hides the impact of the extracting approaches (15.5%). This is true for other cases. The systematic results have revealed a general trend. The larger the initial temperature difference, the more pronounced the impact of the extracting approach.

We also considered three cases presented by Jeon *et al.* [24], using a temperature of 80–1000 eV and a density of 10^{22} – 10^{23} cm^{-3} . It is found that the influence of the extracting approach is trivial such that it can be properly neglected, which is similar when increasing the temperature and its difference. It should be mentioned that Jeon *et al.* [24] used the partial relaxation dynamics (denoted by S₂ here), which is as accurate as the optimal fitting results (S₃) in Table I. In addition, two cases from Dimonte *et al.* [25] have also been recalculated and we observed similar results.

TABLE II. Electron-proton energy relaxation rate ω_{ei} [in units of $W/(K m^3)$]. For dense hydrogens, plasma parameters are consistent with those used by Glosli *et al.* [23], Jeon *et al.* [24], and Dimonte *et al.* [25]. Results are shown only for the S_1 and S_3 methods (the sixth and seventh columns) because S_2 is basically identical to the S_3 method, as can be seen in Table I. The numbers included in brackets denote the power of 10. The last column, defined as $\Delta = |\omega_{ei}(S_1) - \omega_{ei}(S_3)|/\omega_{ei}(S_3)$, indicates the deviation of the S_1 from S_3 method. The number density of electrons (n_e), initial electron (T_e^0), and ion (T_i^0) temperatures are arranged into the third to fifth columns.

Source	Case	n_e cm ⁻³	T_e^0 eV	T_i^0 eV	ω_{ei}		Δ
					S_1	S_3	
Ref. [23]	1		10	20	0.32(14)	0.38(14)	15.5%
	2	10^{20}	30	60	0.82(13)	1.02(13)	19.4%
	3		100	200	0.17(13)	0.23(13)	24.3%
	4		10	20	0.12(18)	0.14(18)	12.2%
	5	10^{22}	30	60	0.48(17)	0.56(17)	15.2%
	6		100	200	0.13(17)	0.16(17)	17.5%
	7		30	60	0.10(21)	0.11(21)	9.8%
	8	10^{24}	100	200	0.50(20)	0.58(20)	15.1%
	9		300	600	0.18(20)	0.22(20)	17.4%
Ref. [24]	1	2.4×10^{22}	80	100	0.103(18)	0.108(18)	4.4%
	2	2.7×10^{23}	400	500	0.143(19)	0.149(19)	4.0%
	3	7.6×10^{23}	800	1000	0.44(19)	0.46(19)	4.3%
Ref. [25]	1	9×10^{20}	15	12	0.16(16)	0.15(16)	6.2%
	2		15	3	0.20(16)	0.16(16)	24.8%

C. Some remarks

In previous sections, we have seen that the impact of the extracting approaches is negligible in some cases, but remarkable in other situations. We also found that it may be related to the initial temperatures and its difference. For a better understanding, we analyze the time-dependent plasma parameter $g(t)$, which is defined as [25] $g(t) = ze^2/\lambda_D(t)k_B T_e(t)$, with $\lambda_D(t)$ being the electronic Debye screening length at time t . The results are shown in Fig. 3 for the cases presented in Table I. To compare them on the same footing, $g(t)$ is normalized

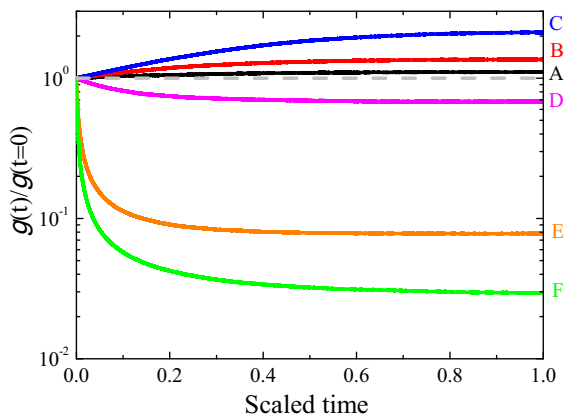


FIG. 3. Plasma parameters g as a function of time for cases A–F analyzed in Table I. For a better comparison, g is normalized by its value at $t = 0$ and the time is scaled to unity. The gray dashed line indicates the normalized plasma parameter equal to 1 at any times.

by its initial value and the evolving time is scaled to unity. Therefore, if $g(t)$ is approaching unity (the gray dashed line), it means that initial plasma properties have been preserved in the energy relaxation process.

In Fig. 3, for cases A–C (fixed T_i^0 and increased T_e^0), the normalized $g(t)$ remains larger than 1, indicating that it relaxes towards much stronger coupled electron-proton plasmas. The situation is reverse for cases D–F (fixed T_e^0 and increased T_i^0) since it is all below unity. Among these cases, case A has nearly preserved the initial plasma properties during the relaxations, so the extracting approach based on the initial plasma parameters, i.e., full relaxation dynamics method (S_1), is still suited for it, which is demonstrated by the results in Table I. Due to energy relaxations, electron-proton plasmas gradually deviate from its initial coupling state; specifically, for cases B and C, the plasmas' coupling is getting enhanced, for which the use of the S_1 method is questionable. The variation of plasma parameter is even more notable for cases D–F. As can be seen, cases E and F rapidly lose the initial plasma coupling. At the thermal equilibrium, the plasma parameter is reduced by more than one order of magnitude.

On the other hand, the DD model [25] has verified a one-to-one correspondence between the electron-proton relaxation rate and the plasma parameter, which allows one to make a rough evaluation on the varying plasma parameters. We select case F as an example. At the scaled time $t = 0, 0.1, 0.2, 0.4, 0.8$, the energy relaxation rate correspondingly attains $(4.2, 0.57, 0.45, 0.38, 0.34) \times 10^{17} W/(K m^3)$, implying that a strong time-varying energy relaxation rate exists. Here, an exponential fitting with a constant energy relaxation rate (S_1) to the MD data, generated by multiple distinct relaxation rates, is thus difficult. In contrast, the partial relaxation dynamics (S_2) and the optimal fitting method (S_3) are more physically motivated since both have reasonably considered the time-dependent nature of the energy relaxation rates during the relaxations. First, the S_2 method avoids the change of the plasmas' coupling strength because the MD simulations have been propagated up to a small fraction of relaxation time, for which an exponential fitting is indeed legitimate for the given plasma conditions. Second, the S_3 method introduces a time-evolving relaxation rate, such that it can perfectly follow the MD data over the entire time span (see Fig. 2), and thus it is reliable to extract the relaxation rates in a wide range of plasma parameters.

Next, we attempt to understand why the initial temperature and its difference matter. We first make a qualitative analysis based on the DD model. By definition, we know that the initial temperature determines the plasma coupling region since $g \propto (T_e^0)^{-1.5}$ is satisfied. The change of energy relaxation rate with respect to g is inversely proportional to g , thereby it is proportional to T_e^0 , i.e., $d\omega_{ei}/dg \propto |1/g| \propto (T_e^0)^{1.5}$, relating the variation of the energy relaxation rate relative to the initial temperature, while the initial temperature difference ($\Delta T = |T_e^0 - T_i^0|$) determines the equilibrium temperature via $T_{eq} = T_i^0 \pm z\Delta T/(z + 1)$, which regulates the coupling of thermalized plasmas.

In order to discriminate the extracting approaches applied in MD simulations, a simple criterion related to the initial plasma temperatures is proposed as follows. It is assumed that the energy relaxation rate during the electron-ion equilibration

does not strongly alter, e.g., $|\omega_{ei}^{\text{init}} - \omega_{ei}^{\text{eq}}|/\omega_{ei}^{\text{init}} \leq \alpha$, where $\omega_{ei}^{\text{init}}$ and ω_{ei}^{eq} denote the relaxation rates at the initial and equilibrium time. α is a small fraction of 1. For $T_i^0 \geq T_e^0$, we can obtain the following relation using the formula of Eq. (1):

$$\left(\frac{T_{\text{eq}}}{T_e^0}\right)^{-\frac{3}{2}} \geq \frac{1-\alpha}{1+\alpha}, \quad (18)$$

where the variation of $\ln \Lambda$ is approximately equal to that of g , which is valid when the initial temperature difference is small. Replacing T_{eq} by the explicit expression in Eq. (13) yields

$$\frac{T_i^0}{T_e^0} \leq \left(\frac{1+\alpha}{1-\alpha}\right)^{\frac{2}{3}} (z+1) - z. \quad (19)$$

In this study, fully ionized hydrogen plasmas are considered, i.e., $z = 1$. If we choose $\alpha = 0.05\text{--}0.1$, it can be further simplified as

$$\frac{T_i^0}{T_e^0} \leq (1.1, 1.3), \quad (20)$$

which means that the full relaxation dynamics method (S_1) is applicable only when the initial temperatures obey this relation, beyond which the S_1 method may result in substantial discrepancies. In Table I, T_i^0/T_e^0 for cases D–F is 1.6, 5.0, and 10.0, respectively, which is much larger than 1.3, so the S_1 method fails in these cases. In Table II, all cases from Ref. [23] retain a constant value of $T_i^0/T_e^0 = 2$, which largely violates the relation given by Eq. (20), and thus the use of the S_1 method here is inappropriate. In contrast, those from Ref. [24] get $T_i^0/T_e^0 = 1.25$, which satisfies the proposed relation, indicating that the S_1 method is still valid, as demonstrated by a small deviation relative to the S_3 method. Similarly, it is straightforward to derive a relation for $T_i^0 \leq T_e^0$.

For a large initial temperature difference, it explores a wide range of plasma couplings during the relaxation, which prohibits us from using a direct exponential fitting method, but satisfactory fitted results can be obtained using an optimal fitting procedure. As discussed above, Eq. (11) behaves excellently to describe electron-ion temperature relaxation; see Fig. 2. If we assume Eq. (2a) is also applicable for a transient plasma, then the following relation holds:

$$v_{ei}(T_e^0) \left(\frac{T_e}{T_e^0}\right)^{-\eta} = v_{ei}(T_e). \quad (21)$$

Insert the explicit expression of v_{ei} , i.e., Eq. (3), into Eq. (21), and it reads

$$\ln \Lambda(T_e) = \left[\frac{(T_i m_e + T_e m_i)}{(T_i^0 m_e + T_e^0 m_i)} \right]^{\frac{3}{2}} \left(\frac{T_e}{T_e^0}\right)^{-\eta} \ln \Lambda(T_e^0), \quad (22)$$

where η can be unambiguously determined for the plasmas considered in this study.

For the cases considered here, case F in Table I traverses a broad coupling regime, which is illustrative to test the derived relation. Using Eq. (22) in case F, it is simple to extrapolate $\ln \Lambda (g < 0.1)$ from its initial value ($g = 0.1$). The present results obtained by a single MD simulation ($\eta = 1$) are shown in Fig. 4. As can be seen, it agrees reasonably well with the independent MD data in Ref. [37] within statistical errors.

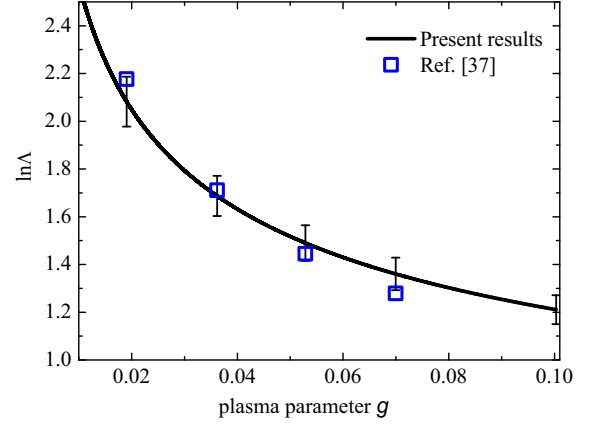


FIG. 4. The Coulomb logarithm ($\ln \Lambda$) vs the plasma parameter (g). The solid curve is computed by a single MD simulation with $n_i = n_e = 3.35 \times 10^{22} \text{ cm}^{-3}$, $T_e^0 = 50 \text{ eV}$, and $T_i^0 = 1000 \text{ eV}$ (case F in Table I). Symbols are independent MD results reported in Ref. [37].

However, its extension into a much broader coupling regime, e.g., evolving from strongly (initial low electron temperature) to weakly coupled plasma, may be limited by the fact that the optimal fitting method is invalid in this case, since a constant η is inadequate.

IV. CONCLUSIONS

In this work, we have used molecular dynamics simulations to investigate energy relaxation processes in weakly-coupled hydrogen plasmas, in which the electron-proton energy relaxation rate is a crucial parameter. To assess it, we have used full and partial relaxation dynamics and optimal fitting methods. Our results have shown that convergent results are available only in particular cases. In most situations considered in this study, the existing extracting approaches yielded results with considerable discrepancies, which are comparable or larger than the variance between analytical models. To our surprise, partial relaxation dynamics and the optimal fitting method produced identical results, i.e., they are convergent regardless of plasma parameters, which has been understood by the evolution of the plasma parameter. To further support our findings, we have reexamined several case studies reported in previous studies [23–25]. In a few cases, it is within statistical errors ($<5\%$). However, in most cases, the impact of the extracting approaches is remarkable with a discrepancy of $\sim 10\%$ – 25% .

To discriminate the use of various methods, we have proposed an empirical, but simple criterion with respect to the initial plasma temperatures. It reveals that the full relaxation dynamics approach may be applicable when a ratio of initial ion temperature to electron is small than 1.3, beyond which other methods should be used for accurate data. Finally, combined with the full relaxation dynamics approach and optimal fitting method, it is possible to extrapolate the Coulomb logarithm of transient electron-proton plasmas in a single MD calculation, which agrees well with previous independent MD data.

Our results are informative to obtain accurate MD-based energy relaxation rates, which may find important applica-

tions in radiation-hydrodynamics simulations. We emphasize that the present results are meaningful for relatively accurate MD simulations, as the statistical error there is negligible. Otherwise, the impact of extracting approaches will be buried under the statistical errors, which is exactly the case in Refs. [17,23,39,40].

ACKNOWLEDGMENTS

We would like to thank the anonymous referees for their valuable comments. Y.W. was funded by the National Natural Science Foundation of China (Grant No. 11934004). C.-B.Z. was financially supported by the National Natural Science Foundation of China (Grant No. 11902041).

APPENDIX: CONVERGENCE ON THE PARTICLE NUMBER

To illustrate the result's convergence on the particle number used in the MD simulations, a typical example for hydrogen plasmas with $n_i = n_e = 10^{23} \text{ cm}^{-3}$, $T_e^0 = 55 \text{ eV}$, and $T_i^0 = 45 \text{ eV}$ is shown in Fig. 5. The number of electrons and ions are simultaneously varied from 10^3 to 10^5 . In line with previous numerical calculations [23], for a given particle number, 10 simulations are run by randomly generating initial positions of particles. Once the simulation is completed, the relaxation time is extracted. In this manner, one can obtain an average relaxation time for 10 simulations as well as its standard deviation, and thereby the Coulomb logarithm with error bars can be acquired.

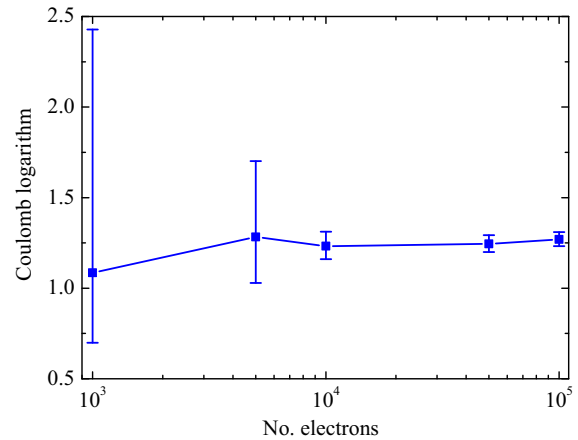


FIG. 5. The Coulomb logarithm ($\ln \Lambda$) vs the number of electrons used in the MD simulations.

It is obvious that the smaller the simulated particle number, the larger the statistical error of MD simulations, as expected. Notably, for 1000 electrons, the absolute deviation is even much larger than the average value, which is qualitatively in agreement with that observed in Ref. [23] (1024 electrons and 1024 ions were used). The tendency towards the convergence is very clear when the number of electrons is increased from 10^3 to 10^4 . The maximum deviation for the number of electrons of 10^4 , 5×10^4 , and 10^5 is 8.0%, 4.9%, and 4.0%, respectively. As a consequence, the number of particles exceeding 10^5 electrons and 10^5 protons is sufficiently numerous in order to yield MD data at a statistically reliable level.

- [1] P. Audebert, R. Shepherd, K. B. Fournier, O. Peyrusse, D. Price, R. Lee, P. Springer, J.-C. Gauthier, and L. Klein, Heating of Thin Foils with a Relativistic-Intensity Short-Pulse Laser, *Phys. Rev. Lett.* **89**, 265001 (2002).
- [2] T. G. White, N. J. Hartley, B. Borm, B. J. B. Crowley, J. W. O. Harris, D. C. Hochhaus, T. Kaempfer, K. Li, P. Neumayer, L. K. Pattison, F. Pfeifer, S. Richardson, A. P. L. Robinson, I. Uschmann, and G. Gregori, Electron-Ion Equilibration in Ultrafast Heated Graphite, *Phys. Rev. Lett.* **112**, 145005 (2014).
- [3] P. M. Leguay, A. Lévy, B. Chimier, F. Deneuille, D. Descamps, C. Fourment, C. Goyon, S. Hulin, S. Petit, O. Peyrusse, J. J. Santos, P. Combis, B. Holst, V. Recoules, P. Renaudin, L. Videau, and F. Dorchie, Ultrafast Short-Range Disorder of Femtosecond-Laser-Heated Warm Dense Aluminum, *Phys. Rev. Lett.* **111**, 245004 (2013).
- [4] P. Celliers, A. Ng, G. Xu, and A. Forsman, Thermal Equilibration in a Shock Wave, *Phys. Rev. Lett.* **68**, 2305 (1992).
- [5] J. R. Rygg, J. A. Frenje, C. K. Li, F. H. Séguin, R. D. Petrasso, D. D. Meyerhofer, and C. Stoeckl, Electron-ion thermal equilibration after spherical shock collapse, *Phys. Rev. E* **80**, 026403 (2009).
- [6] J. D. Lindl, Development of the indirect-drive approach to inertial confinement fusion and the target physics basis for ignition and gain, *Phys. Plasmas* **2**, 3933 (1995).
- [7] D. Riley, N. C. Woolsey, D. McSherry, I. Weaver, A. Djaoui, and E. Nardi, X-Ray Diffraction from a Dense Plasma, *Phys. Rev. Lett.* **84**, 1704 (2000).
- [8] S. P. Hau-Riege, A. Graf, T. Döppner, R. A. London, J. Krzywinski, C. Fortmann, S. H. Glenzer, M. Frank, K. Sokolowski-Tinten, M. Messerschmidt, C. Bostedt, S. Schorb, J. A. Bradley, A. Lutman, D. Rolles, A. Rudenko, and B. Rudek, Ultrafast Transitions from Solid to Liquid and Plasma States of Graphite Induced by X-Ray Free-Electron Laser Pulses, *Phys. Rev. Lett.* **108**, 217402 (2012).
- [9] N. Hartley, P. Belancourt, D. Chapman, T. Döppner, R. Drake, D. Gericke, S. Glenzer, D. Khaghani, S. LePape, T. Ma *et al.*, Electron-ion temperature equilibration in warm dense tantalum, *High Energy Density Phys.* **14**, 1 (2015).
- [10] B. I. Cho, T. Ogitsu, K. Engelhorn, A. Correa, Y. Ping, J. Lee, L. J. Bae, D. Prendergast, R. Falcone, and P. Heimann, Measurement of electron-ion relaxation in warm dense copper, *Sci. Rep.* **6**, 18843 (2016).
- [11] R. T. Sprenkle, L. Silvestri, M. Murillo, and S. Bergeson, Temperature relaxation in strongly-coupled binary ionic mixtures, *Nat. Commun.* **13**, 15 (2022).
- [12] S. Anisimov, B. Kapeliovich, T. Perelman *et al.*, Electron emission from metal surfaces exposed to ultrashort laser pulses, *Sov. Phys. JETP* **39**, 375 (1974).
- [13] J. M. Taccetti, R. P. Shurter, J. P. Roberts, J. F. Benage, B. Graden, B. Haberle, M. S. Murillo, B. Vigil, and F. J. Wysocki,

- An experiment to measure the electron-ion thermal equilibration rate in a strongly coupled plasma, *J. Phys. A: Math. Gen.* **39**, 4347 (2006).
- [14] Y. Maron, Experimental determination of the thermal, turbulent, and rotational ion motion and magnetic field profiles in imploding plasmas, *Phys. Plasmas* **27**, 060901 (2020).
- [15] L. Landau, Kinetic equation for the Coulomb effect, *Phys. Z. Sowjetunion* **10**, 154 (1936).
- [16] L. Spitzer, *Physics of Fully Ionized Gases* (Interscience, New York, 1962).
- [17] J. Hansen and I. McDonald, Thermal relaxation in a strongly coupled two-temperature plasma, *Phys. Lett. A* **97**, 42 (1983).
- [18] M. W. C. Dharma-wardana and F. Perrot, Energy relaxation and the quasi-equation of state of a dense two-temperature nonequilibrium plasma, *Phys. Rev. E* **58**, 3705 (1998).
- [19] G. Hazak, Z. Zinamon, Y. Rosenfeld, and M. W. C. Dharma-wardana, Temperature relaxation in two-temperature states of dense electron-ion systems, *Phys. Rev. E* **64**, 066411 (2001).
- [20] D. O. Gericke, M. S. Murillo, and M. Schlanges, Dense plasma temperature equilibration in the binary collision approximation, *Phys. Rev. E* **65**, 036418 (2002).
- [21] L. S. Brown, D. L. Preston, and R. L. Singleton Jr, Charged particle motion in a highly ionized plasma, *Phys. Rep.* **410**, 237 (2005).
- [22] M. S. Murillo and M. W. C. Dharma-wardana, Temperature Relaxation in Hot Dense Hydrogen, *Phys. Rev. Lett.* **100**, 205005 (2008).
- [23] J. N. Glosli, F. R. Graziani, R. M. More, M. S. Murillo, F. H. Streitz, M. P. Surh, L. X. Benedict, S. Hau-Riege, A. B. Langdon, and R. A. London, Molecular dynamics simulations of temperature equilibration in dense hydrogen, *Phys. Rev. E* **78**, 025401(R) (2008).
- [24] B. Jeon, M. Foster, J. Colgan, G. Csanak, J. D. Kress, L. A. Collins, and N. Grønbech-Jensen, Energy relaxation rates in dense hydrogen plasmas, *Phys. Rev. E* **78**, 036403 (2008).
- [25] G. Dimonte and J. Daligault, Molecular-Dynamics Simulations of Electron-Ion Temperature Relaxation in a Classical Coulomb Plasma, *Phys. Rev. Lett.* **101**, 135001 (2008).
- [26] L. X. Benedict, J. N. Glosli, D. F. Richards, F. H. Streitz, S. P. Hau-Riege, R. A. London, F. R. Graziani, M. S. Murillo, and J. F. Benage, Molecular Dynamics Simulations of Electron-Ion Temperature Equilibration in an SF₆ Plasma, *Phys. Rev. Lett.* **102**, 205004 (2009).
- [27] J. Daligault and G. Dimonte, Correlation effects on the temperature-relaxation rates in dense plasmas, *Phys. Rev. E* **79**, 056403 (2009).
- [28] J. Vorberger, D. O. Gericke, T. Bornath, and M. Schlanges, Energy relaxation in dense, strongly coupled two-temperature plasmas, *Phys. Rev. E* **81**, 046404 (2010).
- [29] S. D. Baalrud and J. Daligault, Effective Potential Theory for Transport Coefficients across Coupling Regimes, *Phys. Rev. Lett.* **110**, 235001 (2013).
- [30] G. Faussurier and C. Blancard, Temperature relaxation in dense plasmas, *Phys. Rev. E* **93**, 023204 (2016).
- [31] J. Daligault and J. Simoni, Theory of the electron-ion temperature relaxation rate spanning the hot solid metals and plasma phases, *Phys. Rev. E* **100**, 043201 (2019).
- [32] Q. Ma, J. Dai, D. Kang, M. S. Murillo, Y. Hou, Z. Zhao, and J. Yuan, Extremely Low Electron-ion Temperature Relaxation Rates in Warm Dense Hydrogen: Interplay between Quantum Electrons and Coupled Ions, *Phys. Rev. Lett.* **122**, 015001 (2019).
- [33] R. A. Baggott, S. J. Rose, and S. P. D. Mangles, Temperature Equilibration due to Charge State Fluctuations in Dense Plasmas, *Phys. Rev. Lett.* **127**, 035002 (2021).
- [34] Y. T. Lee and R. More, An electron conductivity model for dense plasmas, *Phys. Fluids* **27**, 1273 (1984).
- [35] J. Vorberger and D. Gericke, Comparison of electron-ion energy transfer in dense plasmas obtained from numerical simulations and quantum kinetic theory, *High Energy Density Phys.* **10**, 1 (2014).
- [36] J. Simoni and J. Daligault, First-Principles Determination of Electron-Ion Couplings in the Warm Dense Matter Regime, *Phys. Rev. Lett.* **122**, 205001 (2019).
- [37] L. X. Benedict, M. P. Surh, J. I. Castor, S. A. Khairallah, H. D. Whitley, D. F. Richards, J. N. Glosli, M. S. Murillo, C. R. Scullard, P. E. Grabowski, D. Michta, and F. R. Graziani, Molecular dynamics simulations and generalized Lenard-Balescu calculations of electron-ion temperature equilibration in plasmas, *Phys. Rev. E* **86**, 046406 (2012).
- [38] L. X. Benedict, M. P. Surh, L. G. Stanton, C. R. Scullard, A. A. Correa, J. I. Castor, F. R. Graziani, L. A. Collins, O. Čertík, J. D. Kress, and M. S. Murillo, Molecular dynamics studies of electron-ion temperature equilibration in hydrogen plasmas within the coupled-mode regime, *Phys. Rev. E* **95**, 043202 (2017).
- [39] C. Blancard, J. Clérouin, and G. Faussurier, Electron-ion temperature relaxation in hydrogen plasmas, *High Energy Density Phys.* **9**, 247 (2013).
- [40] Q. Ma, J. Dai, D. Kang, Z. Zhao, J. Yuan, and X. Zhao, Molecular dynamics simulation of electron-ion temperature relaxation in dense hydrogen: A scheme of truncated Coulomb potential, *High Energy Density Phys.* **13**, 34 (2014).
- [41] J. Gao, Y. Wu, Z. Zhong, and J. Wang, The influence of density in ultracold neutral plasma, *Phys. Plasmas* **23**, 123507 (2016).
- [42] N. R. Shaffer and S. D. Baalrud, The Barkas effect in plasma transport, *Phys. Plasmas* **26**, 032110 (2019).
- [43] F. Zhou, Y. Qu, J. Gao, Y. Ma, Y. Wu, and J. Wang, Atomic-state-dependent screening model for hot and warm dense plasmas, *Commun. Phys.* **4**, 148 (2021).
- [44] S. Baalrud and J. Daligault, Temperature anisotropy relaxation of the one-component plasma, *Contrib. Plasma Phys.* **57**, 238 (2017).
- [45] B. Xu and S. X. Hu, Effects of electron-ion temperature equilibration on inertial confinement fusion implosions, *Phys. Rev. E* **84**, 016408 (2011).
- [46] Z. Fan, J. Liu, B. Liu, C. Yu, and X. He, Ignition conditions relaxation for central hot-spot ignition with an ion-electron non-equilibrium model, *Phys. Plasmas* **23**, 010703 (2016).
- [47] Z. Fan, Y. Liu, B. Liu, C. Yu, K. Lan, and J. Liu, Non-equilibrium between ions and electrons inside hot spots from National Ignition Facility experiments, *Matter Radiat. Extrem.* **2**, 3 (2017).
- [48] G. Dimonte, Quantitative metrics for evaluating thermonuclear design codes and physics models applied to the National Ignition Campaign, *Phys. Plasmas* **27**, 052709 (2020).

- [49] S. Plimpton, Fast parallel algorithms for short-range molecular dynamics, *J. Comput. Phys.* **117**, 1 (1995).
- [50] T. Dunn and A. A. Broyles, Method for determining the thermodynamic properties of the quantum electron gas, *Phys. Rev.* **157**, 156 (1967).
- [51] H. Minoo, M. M. Gombert, and C. Deutsch, Temperature-dependent Coulomb interactions in hydrogenic systems, *Phys. Rev. A* **23**, 924 (1981).
- [52] T. Schneider and E. Stoll, Molecular-dynamics study of a three-dimensional one-component model for distortive phase transitions, *Phys. Rev. B* **17**, 1302 (1978).